RESEARCH PAPER

Wound healing promotion by poly(vinyl alcohol)/chitosan electrospun nanofibrous scaffold loaded with *Achillea wilhelmsii* extract

Omid Tavallaei [1], Mahtab Doostan [2], Kamyar Khoshnevisan [3, 4], Ali Tahmasebi [2], Hassan Maleki [1, 2]*

[1]*Pharmaceutical Sciences Research Center, Health Institute, Kermanshah University of Medical Sciences, Kermanshah, Iran*
[2]*Student Research Committee, Kermanshah University of Medical Sciences, Kermanshah, Iran*
[3]*Medical Nanotechnology and Tissue Engineering Research Center, Shahid Beheshti University of Medical Sciences, Tehran, 1983963113, Iran*

ABSTRACT

Objective(s): Natural component-included scaffolds can provide numerous benefits for skin healing and tissue regeneration. Nanofibers (NFs) with intricately intertwined three-dimensional structures afford an exclusive matrix for delivering therapeutics. This research assessed nanofibrous scaffolds loaded with *Achillea wilhelmsii* extract (5-15 wt%) for skin tissue engineering.
Materials and Methods: *A. wilhelmsii*-loaded scaffolds, composed of poly(vinyl alcohol) (PVA) and chitosan (CS), were fabricated by the electrospinning process. Subsequently, the physicochemical properties of the scaffolds were evaluated through relevant analyses. The antioxidant activity and degradation rate of the scaffolds were also determined. Cell viability and scratch assays on dermal fibroblasts were conducted to assess proliferation and migration activities.
Results: Electron micrographs revealed interconnected fibers with a nano-scale diameter (> 400 nm) and uniform morphology. Additionally, the intact presence of *A. wilhelmsii* extract in the polymeric matrix was confirmed without any undesirable interactions. The proposed scaffolds verified favorable mechanical properties, a hydrophilic nature, high volume porosity (>90%), and water absorption capability (<500%). Besides, the findings demonstrated the remarkable radical scavenging ability of *A. wilhelmsii* extract in the nanofibrous scaffolds, along with controlled degradation kinetics over 72 h. The viability assay proved that the *A. wilhelmsii*-loaded scaffolds not only exhibited no cytotoxicity but also improved cell proliferation. The scaffolds also significantly accelerated fibroblast migration and complete closure of scratched areas.
Conclusion: At last, the obtained results revealed that *A. wilhelmsii*-loaded PVA/CS NFs can be applied as a potential scaffold for skin regeneration and wound healing promotion.

Keywords: *Antioxidants, Electrospinning, Nanofibers, Tissue scaffolds, Wound healing*

INTRODUCTION

The skin, as the largest body part in the human, plays a critical role in safeguarding against bacterial and viral pathogens, facilitating tactile sensations, and regulating the body's thermoregulatory processes [1, 2]. The human integumentary system encompasses three primary layers: the epidermis, dermis, and hypodermis. These layers are susceptible to numerous potential afflictions, including the development of cancerous lesions, formation of acne, and occurrence of various types of wounds [3]. Severe and chronic skin injuries, especially profound woundscan lead to significant morbidity and mortality [4]. The management of injuries and wound repair relies heavily on being timely and efficient. The wound healing process in humans and animals occurs through a highly intricate and sophisticated mechanism, comprising

---

successive phases of hemostasis, inflammation, proliferation, restoration, and reconstruction [5, 6]. However, various pathological and pathogenic conditions can retard and impede the normal wound healing process.

Noteworthy attention has been focused on reducing the burden caused by wounds by discovering novel wound care techniques and speeding up the healing process. The emphasis has been on discovering innovative therapeutic methods and continuously improving technologies to effectively manage both acute and chronic wounds [7]. Exploiting wound dressings is one of the main strategies for preventing infection, and maintaining the wounds adequately moist [8]. Likewise, wound dressings should be biocompatible, non-toxic, non-allergenic, removable, and non-adherent to the wound. They should also provide the capability to enhance epidermal proliferation and migration [9]. Extensively investigated wound dressings include different types of gauzes, transparent films, foam dressings, hydrogels, and hydrocolloids. While each of these options offers several benefits, certain drawbacks have remained relatively consistent, such as poor antimicrobial and mechanical properties [10].

Nanofibers (NFs), a novel type of wound dressing, have been recognized as a dynamic class of one-dimensional nanomaterials with incomparable physicochemical characteristics. These structures possess high surface-to-area ratios, porosity, and permeability, enabling them to absorb moisture and exudate while facilitating the exchange of oxygen, water, and nutrients [11]. NFs can also function as reservoirs or delivery systems for loaded therapeutic agents, allowing them to effectively prevent degradation before reaching their target sites, thus diminishing side effects [12]. The electrospun nanofibrous structures render a distinctive architecture and mirror biological characteristics similar to the structure of the extracellular matrix (ECM) [13]. Numerous techniques are available for producing NFs, with electrospinning having emerged as the most widely exploited methodology.

Electrospinning is a technique through which non-woven nanofibrous scaffolds are produced from a polymer solution by applying an electric field [14]. Electrospun nanofibrous structures are predominantly fabricated using natural and synthetic polymers, or a combination thereof, to attain boosted properties [14].

Polyvinyl alcohol (PVA) is one of the most widely used synthetic polymers for producing NFs. PVA as a semi-crystalline, hydrophilic, cytocompatible, biodegradable, easy-to-process and non-toxic polymer [15, 16], has significant water permeability [17]. In addition, electrospun PVA NFs hold great promise for use as drug delivery carriers and wound dressing applications [18]. Besides, it can be co-polymerized with various polymers, leading to enhanced physicochemical characteristics of NFs [19]. Notably, chitosan (CS) has been documented as a polymer that can complete this outcome.

CS, a cationic biopolymer derived from chitin, has garnered interest owing to its unique structural properties and biological applications. CS is obtained through the alkaline deacetylation of chitin [20]. The distinguished attributes of CS include biocompatibility, biodegradability, and plasticity, along with its capacity to undergo hydrolysis within lysosomes, assisting wound healing. Moreover, this polymer displays antibacterial activities, enhanced cellular function, and reduced inflammatory responses during the process of repairing the affected region [21]. The mechanical properties of CS are remarkably enhanced through blending with PVA due to their distinct intermolecular interactions [22].

Nowadays, herbal medicine-derived products have been employed in treating skin injuries due to their reasonable therapeutic impacts on wound healing. Numerous plant species have been considered for their potential in wound healing and tissue engineering applications. Among these, *Achillea wilhelmsii* C. Koch (*A. wilhelmsii*), a member of the Asteraceae family, is commonly applied as a traditional medicine. *A. wilhelmsii* is one of the most well-known *Achillea* species, typically found in Iran and the Middle East. The prominent active components identified in *A. wilhelmsii* include flavonoids, polyphenols, monoterpenes, and sesquiterpenes [23–25]. Thanks to the high content of these components, diverse pharmacological activities have been attributed to them, including antioxidant, anti-inflammatory, and antimicrobial properties. As a result, it has been employed in the treatment of various conditions such as skin wounds, infections, gastrointestinal ulcers, hemorrhages, and pneumonia [23]. Despite the various biological attributes of *A. wilhelmsii*-derived products, its oral administration has been restricted due to several obstacles, including acidic

and enzymatic degradation, first-pass metabolism, and poor absorption [26]. Whereas, localized and controlled delivery systems, such as NFs-based systems, can overcome these obstacles [27]. In one study, *Achillea millefolium* (AM) and Viola (V) extracts have been considered for emerging biocompatible CS/PVA electrospun NFs. The results revealed that Viola extract displayed great mechanical properties, antibacterial efficacy, and enhanced wound closure [28].

The present investigation aims to harness the biological activities of *A. wilhelmsii* extract in conjunction with the unique attributes of NFs to promote skin regeneration and wound healing. To this end, electrospun NFs, composed of PVA and CS polymers, loaded with *A. wilhelmsii* extract were produced and subsequently characterized in terms of their physicochemical properties. The antioxidant activity, degradation rate, and release profile were then determined. Finally, *in-vitro* studies on cell proliferation and cell migration were conducted to unveil the potential for wound healing promotion.

MATERIALS AND METHODS
Materials

PVA (Mw = 72 KDa, Hy = 99.5%) and CS (Mw: 50-190 KDa, 75–85% deacetylated) were purchased from Sigma-Aldrich (Germany). Acetic acid, ethanol, dimethyl sulfoxide (DMSO), and 2,2-diphenyl-1-picrylhydrazyl (DPPH, 95%) were procured from Merck Company (Darmstadt, Germany). The materials used for cell studies were obtained from Gibco (Marcq-enBarœul, France), including Dulbecco's modified Eagle's medium (DMEM) high glucose, fetal bovine serum (FBS), 3-(4,5-dimethylthiazol-2-yl-2,5-diphenyltetrazolium bromide) (MTT), 0.05% trypsin/EDTA, and phosphate buffer saline (PBS). All other chemical solvents applied in the experiments were of analytical grade.

A. wilhelmsii extraction

To prepare a hydro-alcoholic extract by maceration method [26, 29], the fresh aerial parts of *A. wilhelmsii* (stems, leaves, and flowers) were collected from Kermanshah province of Iran in the blooming season. The taxonomic identification was confirmed by a pharmacognostic. First, they were cleaned, dried in the shade, homogenously ground, and then immersed in 70% ethanol in a shaker for 72 hr at 25 °C. The obtained mixture

was filtered using filter paper Whatman No. 42. Following, it was dehydrated in a rotary evaporator at 40 °C for 24 hr. Ultimately, the concentrated extract was gathered and stored at 4 °C for the subsequent studies.

Fabrication of A. wilhelmsii-loaded electrospun NFs

The bare PVA/CS NFs and *A. wilhelmsii*-loaded NFs were fabricated by electrospinning technique, as previously reported [30]. Initially, CS was dissolved in acid acetic (1 %) at the concentration of 2% w/v, and PVA was dissolved into distilled water at 10% w/v. Then, they were blended at the ratio of 80:20 v/v and subjected to electrospinning to prepare the bare PVA/CS NFs. Similarly, 5-20 wt% (5, 10, 15, and 20% w/w) of *A. wilhelmsii* extract was added to the PVA/CS mixture, and electrospun fibers were acquired at room temperature (25 °C).

The electrospinning process was set at a constant flow rate of 1 mL/hr, the electric field strength was 18 kV, and the needle tip-to-collector distance was 18 cm. After electrospinning, the resultant scaffolds were detached from the metal drum and preserved for further characterization and experiments.

Diameter and morphology characterization

The diameter and morphological analysis of the proposed NFs was carried out through scanning electron microscopy (SEM, DSM 960A, Zeiss, Oberkochen, Germany). The imaging was conducted at an accelerating voltage of 30.0 kV after gold sputtering the surface of the samples. Besides, Image J software was applied to calculate the average diameter of samples by measuring the diameter of 100 randomly selected fibers per microscopic image.

Infrared spectroscopy analysis

The chemical structure of the extract and its presence in the NFs were analyzed by Fourier transform infrared (FTIR) spectrophotometer (Shimadzu IRAffinity-IS; Shimadzu, Kyoto, Japan). Spectra was recorded in the absorbance mode from 400 to 4000 cm^{-1} at room temperature.

Antioxidant activity

The antioxidant properties of various samples including the extract, and extract-loaded NFs were evaluated by using the scavenging DPPH free radical technique [31].

Briefly, altered concentrations of the samples were dispersed together with 10-4 M DPPH in 4 mL of ethanol. Then, the prepared mixtures were incubated under shaking in the dark for 60 min at room temperature (25 ± 1°C). After that, the absorbance of the resultant dispersions was examined by UV-Vis spectrometer at 517 nm. Based on the following equation, the percentage of antioxidant activity was calculated:

Antioxidant activity (%) = [(Ac - As)/Ac] × 100

where Ac is the absorbance of DPPH solution without samples, and As is the absorbance of DPPH solution in the presence of samples.

Wettability, water absorption capacity, and porosity measurement

The surface wettability of the prepared nanofibrous mats was measured using the sessile drop technique with a contact angle meter (G10, KRUSS, Germany). The proposed scaffolds were affixed to a glass slide, and 4 μL of distilled water was dispensed onto the surface of each sample. Subsequently, imaging was carried out immediately, and the contact angle value was measured.

The nanofibrous scaffolds were immersed in PBS (pH 7.4) at 37 °C to determine the water absorption capacity. Initially, the dry weight of the samples (Wd) was measured after specific incubation times that they were removed from the medium. Then, they were situated on tissue paper to drain off the excess water. Following, the samples were weighed as the wet weight (Ww). The W was expressed as the water absorption percentage and calculated in the given equation:

W = [(Ww - Wd)/Ww] × 100%

The prepared scaffolds' porosity was measured via the liquid displacement method [32]. To do so, the volume of a specific amount of ethanol was initially calculated (V1), and the sample was then immersed in it. After a 1 hr immersion, the volume was measured (V2), and the sample was subsequently eliminated. To end, the volume of the solution without the sample (V3) was determined, and the porosity percentage of the samples was calculated using the following formula:

Porosity (%) = [(V1 - V2)/(V2 - V3)] × 100

Mechanical strength analysis

The mechanical properties of the bare and loaded scaffolds were analyzed using a tensile strength tester (Santam, Tehran, Iran). The samples with dimensions of 30×50 mm^2 were fixed between two clamps of the instrument, and the stretching rate was maintained at 2 mm/min under a load cell of 10 N. The stress-strain curves were recorded, and mechanical parameters were determined.

In-vitro degradation study

The degradation of the scaffolds was evaluated by immersing the samples in a dimension of 3×3 cm^2 into 50 mL of PBS (0.01 M, pH 7.4). They were placed in a shaker-incubator under shaking (100 rpm/min) at 37 °C. Then, the samples were omitted from the solutions at specified times, dried in a vacuum dryer, and weighed after complete drying. The degradation rate at each time point was determined by comparing the weight before and after the immersion of specimens, as follows:

Weight loss (%) = [(Wi-Wt)/Wi] × 100

where Wi is the initial weight of the samples, and Wt is the weight after drying at each time point.

Cell viability measurement

The viability of human dermal fibroblast (HDF) cells, which play a crucial role in cutaneous wound healing, on the nanofibrous scaffolds was determined using direct MTT colorimetric assay. The bare PVA/CS scaffold and PVA/CS scaffolds containing 5-15 wt% *A. wilhelmsii* extract were cut into circular disk shapes of 10 mm in diameter and sterilized with UV light for 2 hr on each side. Then, they were layered over the 48-well culture plates, and HDF cells (10,000 per well) were seeded on the plates in the DMEM/high-glucose medium containing 10 % FBS and 1 % penicillin/streptomycin in a humidified incubator at 37 °C with 5 % CO$_2$. After that, the plates were incubated for 24 hr and 48 hr. Likewise, HDF cells seeded into the wells without any scaffold were set as the control group. After the elapsed incubation time, cell mediums were discarded, the cells were washed with PBS, and 100 μL of 0.5 mg/mL MTT aqueous solution was added to each well and incubated for 4 hr. Next, the media was removed, and DMSO was added to dissolve the purple-colored formed formazan crystals. Finally, absorbance was measured at 570 nm using a plate reader and the percentage cell viability was calculated as follows:

Cell viability (%) = [OD of the test sample/OD of the control] × 100

In-vitro cell migration assay

Scratch assay was used to assess the fibroblasts'

capacity for migration and wound closure as one of the most critical stages of wound healing [33, 34]. To achieve this, HDF cells were cultivated into a 24-well plate at 50,000 cells/well and then were incubated at 37 °C for 24 hr to form a cell monolayer with high confluency (> 80 %). Also, a serum-free medium holding mitomycin C (5 g/mL) was added to the wells to inhibit cell proliferation, the medium was discarded, and the wells were washed with PBS. Later, the middle of the HDF monolayer with a micropipette tip was scratched to create linear wounds with a cell-free zone. Subsequently, both UV light-sterilized bare and loaded scaffolds were placed in the wells over the mediums without touching the cell monolayers. In addition, the control group was considered as an untreated monolayer of scratched cells in the complete medium. The wound closure rate was observed and photographed using a light microscope at 0 hr, 24 hr, and 48 hr after scratching. Finally, the unfilled wound area was manually estimated by Image J software at the appointed times. The following formula was used to determine the rate of wound closure:

Rate of wound closure (%) = [(A0 - At)/A0] × 100

A0 represents the initial wound, and At represents the wound at the appointed time.

Statistical analysis

The measured data were described as the mean ± standard deviation (n=3). Statistical analysis was implemented using one- or two-way analysis of variance (ANOVA) by GraphPad Prism 9 software. The value of $P < 0.05$ was considered statistically significant.

RESULTS AND DISCUSSIONS
Diameter and morphological characterizations

Nanofibrous scaffolds can mimic natural architecture in terms of size and morphology. In addition, such scaffolds are capable of being loaded with natural substances to promote cell activities, e.g., adhesion, proliferation, and migration. Therefore, an electrospun PVA/CS scaffold was constructed and loaded with three amounts of *A. wilhelmsii* extract. In this regard, the bare and loaded fibers were microscopically analyzed, as depicted in Fig. 1. The PVA/CS scaffold indicated a porous structure having a uniform morphological structure without beads with a diameter distribution of 324 ± 65 nm (Fig. 1a). After adding *A. wilhelmsii* extract (5 wt%), the uniform and bead-free NFs were shaped, and the diameter was augmented to an average of 378 ± 70 nm (Fig. 1b). The further addition of the extract (10 wt%) produced the smooth NFs with a relatively uniform shape and morphology with a slightly higher diameter of 395 ± 68 nm (Fig. 1c). Whereas increasing the extract to 15 wt% made a blend of interconnected flat and ribbon-shaped NFs with a slightly smaller average diameter and
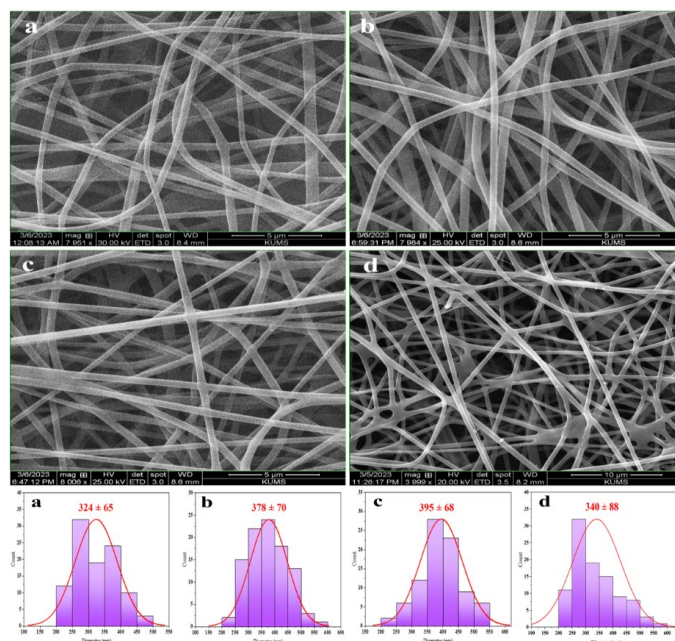
Fig. 1. SEM micrograph of bare PVA/CS NFs (a) and NFs containing 5, 10, and 15 wt% *A. wilhelmsii* extract (b-d) with the corresponding fiber diameter distribution histograms below them (The scale bar was 5 μm for a-c and 10 μm for d)

wider size distribution (340 ± 88 nm, Fig. 1d). This outcome could be attributed to the insufficient viscosity of the electrospinning solution and lower entanglement of the polymer's chains [31, 35]. The higher amount of extracts (>10 wt%) induced non-hemogenous fibers in formation comprising the structural faults e.g., beads and drops, which might lessen the dynamic surface area of electrospun NFs and touch the release profile [36, 37]. As a result, using higher amounts of the extract (> 15 wt%) resulted in the generation of weaknesses in fiber morphology and diameter, which is why these conditions were not selected for further experiments.

FTIR characterization

The chemical structure of the materials used in the scaffolds and presence of *A. wilhelmsii* extract were inspected by FTIR spectroscopy (Fig. 2). The spectrum of bare PVA/CS NFs indicated the characteristic peaks related to the functional groups of PVA and CS polymers at 842 cm^{-1}, 1091 cm^{-1}, 1249 cm^{-1}, 1730 cm^{-1}, 2910 cm^{-1}, and 3280 cm^{-1}, assigned to the C–C, C–O, C–N, C=O, C–H, and O–H bonds, respectively [30, 34]. Though the spectra associated with CS may be disappeared in PVA spectra, the polymers did not have a negative effect on each other and stayed intact during the process [30]. Moreover, *A. wilhelmsii* extract appeared to have typical absorbance peaks derived from the accessible compounds, mostly terpenoids and flavonoids, at 1060 cm^{-1} (C–O stretching), 1267 cm^{-1} (C–N stretching), 1384 cm^{-1} (–CH3 bending), 1622 cm^{-1} (C=O stretching), 2926 cm^{-1} (–CH scratching), and a broad peak at 3200–3600 cm^{-1} relating to overlapped N–H and O–H scratching bonds [27, 35]. By integrating *A.*

wilhelmsii extract in PVA/CS scaffold, the noticeable distinctive peaks of the extract and PVA/CS NFs appeared in the spectrum with a minor shift in peaks and the change in their intensities [26, 38]. It is perhaps attributed to the physical association between the functional groups of polymers and the extract components. These results imply the intact presence of polymers and the extract in the matrix of the NFs without any undesirable interaction.

Antioxidant activity

Oxidative stress and oxidant free radicals are predominantly involved in decelerating and impairing wound healing and tissue regeneration processes, principally in chronic non-healing wounds [39]. Hence, antioxidant components can support the control of these processes by cleansing and inactivating reactive oxygen species (ROS) [40]. As shown in Fig. 3, the free *A. wilhelmsii* extract showed DPPH scavenging activity of 41% to 93% at 25-400 µg/mL. The average scavenging activity of *A. wilhelmsii*-loaded nanofibrous scaffolds (5 wt%) was around 24–65% with a statistically significant difference compared to the free extract. Moreover, the extract-loaded NFs (10 wt%) provided 38% scavenging activity at 25 µg/mL and reached a peak of 79% at 400 µg/mL, indicating the extract was incorporated into the scaffold. At the same concentrations, the extract-loaded NFs (15 wt%) supplied 39-86 % antioxidant activity without statistical difference compared to the free extract and the loaded NFs (10 wt%) (P>0.05). These findings confirmed the remarkable radical scavenging capability of *A. wilhelmsii* extract, also preserved in the nanofibrous scaffolds. The antioxidant activity is
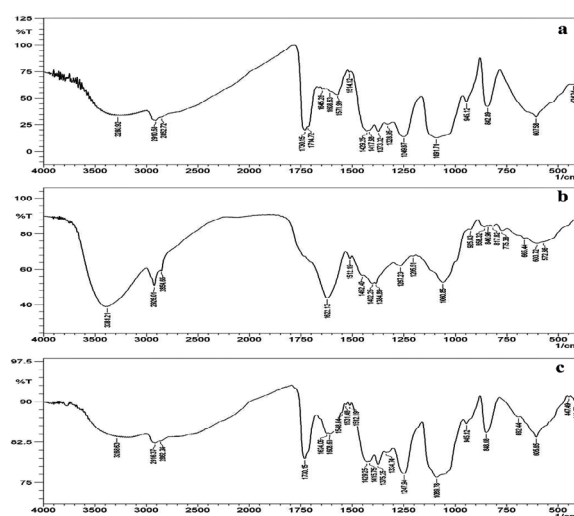
Fig. 2. FTIR spectrum of bare PVA/CS scaffold (a), A. wilhelmsii extract (b), and A. wilhelmsii-loaded PVA/CS scaffold (c).
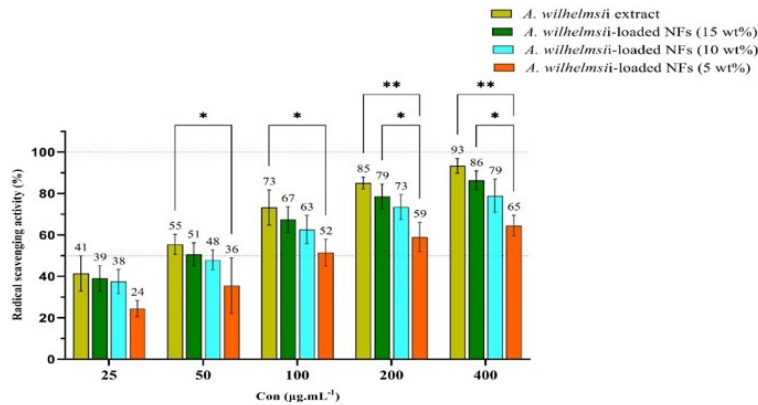
Fig. 3. DPPH radical scavenging activity of A. wilhelmsii extract and the PVA/CS scaffolds containing 5, 10, and 15 wt% extract (* represents P<0.05, ** represents P<0.01)

attributed to the bio-compounds present in the extract, such as trans-carveol, linalool, camphor, etc., that enable the inhibition and deactivation of oxidative stress reactions generated by ROS during wound healing process [23, 39, 41, 42]. Antioxidant features of natural compounds can be associated with oxidation prevention mechanism of bioactive molecules' and consequently, confer remarkable defense against stress linked to syndromes [43]. Antioxidant compounds in a reasonable concentration can also considerably speed up wound healing process [44].

Porosity, wettability, and water absorption capability

A desirable scaffold for wound healing purposes should possess high porosity to allow permeability for the diffusion of oxygen and nutrients as well as facilitate cellular infiltration, proliferation, and migration [45]. The porosity measurement of bare PVA/CS scaffolds clarfied an average value of 95 %, while the loading of 5, 10, and 15% A. wilhelmsii extract resulted in the value of 93.6%, 92.1%, and 90.1% porosity of the total scaffold volume, respectively (Fig. 4a). These results endorsed the high porosity of scaffolds and the extract loading
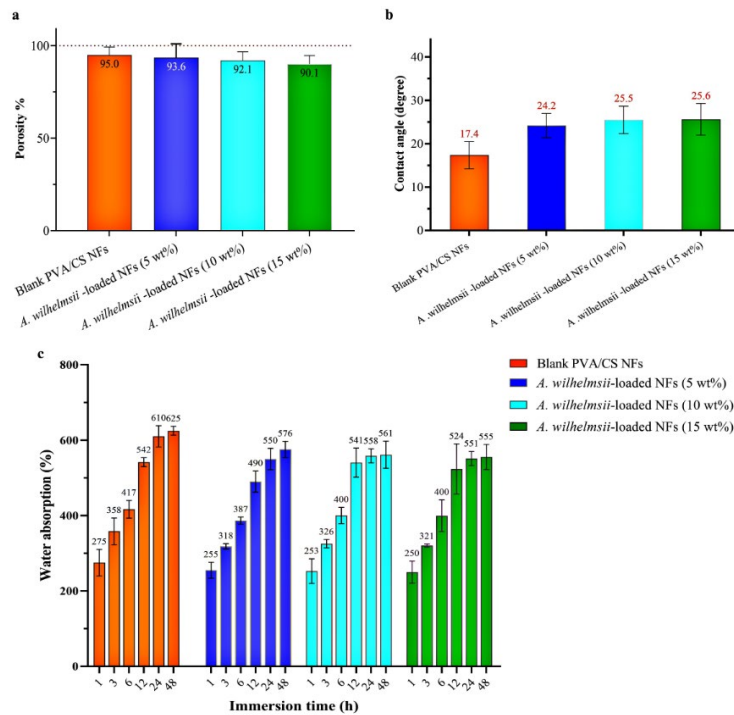
Fig. 4. The percentage of porosity (a), value of water contact angle (b), and water absorption capacity (c) of bare and A. wilhelmsii-loaded scaffolds (Average values are indicated above the columns).

had no significant impact on the amount of porosity. Likewise, SEM images indicate the nano-scale pore size with high interconnection desirable for the permeability of gases/nutrients and tissue regeneration.

The surface hydrophilicity of the nanofibrous scaffolds is of paramount importance, as it influences cell adhesion, proliferation, and spreading, along with the absorption of wound fluids/exudates and control of moisture loss during wound healing [39, 40]. Moreover, wettability of wound dressing is an essential part of conserving tissue moisture during healing process of a wound [46]. As an indicator of hydrophilicity, the contact angle of scaffolds was measured, and the relevant values were presented in Fig. 4b. The bare scaffold exhibited a contact angle of 17.4 ± 3.1º, indicating the scaffold surface's high wettability and hydrophilic nature. Further, the loading of *A. wilhelmsii* extract slightly increased the contact angle values to reach 24.1 ± 2.8º, 25.5 ± 3.2º, and 25.6 ± 3.6º after 5, 10, and 15 % extract, successively. Also, all scaffolds' contact angles reached 0º after 10 s. Although the extract inclusion into scaffolds elevated the contact angle value, they were not statistically significant compared to the bare scaffold.

Fig. 4c depicts the water absorption capability of the obtained scaffolds. The bare PVA/CS scaffold revealed that water uptake was about 275% after 1 hr immersion and 625% after 48 hr immersion. In comparison, the extract-loaded scaffolds (5-15%) showed roughly 250% water uptake and reached 576%, 561%, and 555% after 48 hr immersion, respectively. This characteristic of the nanofibrous scaffolds suggests that they could absorb a high content of secretions/exudates and maintain moisture at the wound site [47, 48].

Owing to hydrogen bonding amid polymeric chains and water, the most hydrogel fibers containing CS and PVA exhibited high water absorbency [46, 49]. The aqueous functional groups in the structure of CS/PVA, for instance amine (NH2), hydroxyl [−OH], and amide (−CONH-, −CONH2) could boost swelling degree of NFs [50].

Mechanical properties

Wound dressing materials would possess sufficient mechanical properties, especially tensile strength, to ensure structural integrity during usage. Thus, the analyses were accomplished to evaluate the effect of the incorporation of *A. wilhelmsii* extract on the mechanical property, as shown in Fig. 5. The bare PVA/CS scaffolds show
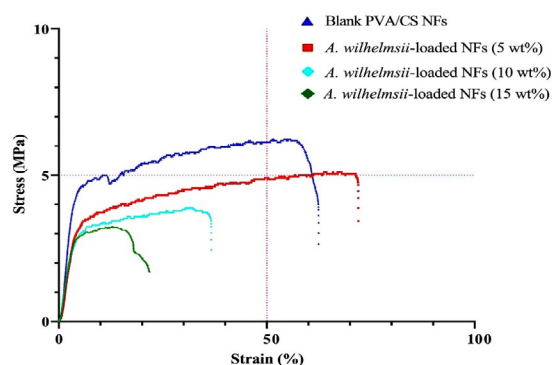
Fig. 5. Representative stress versus strain curve of the obtained nanofibrous scaffolds

that the average values of 11.2 MPa, 6.2 MPa and 55.8 % for tensile modulus, ultimate tensile stress, and strain, respectively, while the subsequent values after adding 5 wt% extract were 7.5 MPa, 5.1 MPa, and 68.1%. The addition of the extract (10 wt%) caused the reduction of ultimate tensile stress and strain to average values of 3.9 MPa and 32.3 %, though these values indicate favorable strength and tensile for cutaneous wound healing application [41]. In addition, the greater incorporation of the extract (15 wt%) resulted in more reduction in the mechanical parameters. This could result from the disruption of the scaffold network by reducing chain entanglements and altering the formation of physical interactions between the functional groups of the extract and the polymer chains [30, 42].

In-vitro degradation studies

The *in-vitro* degradation rate of the scaffolds is shown in Fig. 6. The bare PVA/CS scaffold loses 34%, 49%, 67%, and 95% of its initial weight after 12 hr, 24 hr, 48h, and 72 hr, respectively, possibly due to the surface/bulk erosion of matrix and hydrolytic cleavage of the polymeric chains [51, 52]. *A. wilhelmsii*-loaded scaffolds (5 wt%) degraded 42% of its initial weight in just 12 hr and close to complete degradation (96%) after 72 hr
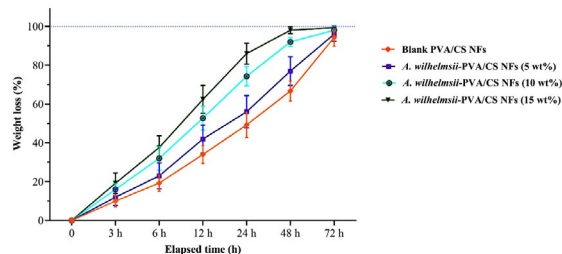
Fig. 6. Degradation behavior of bare PVA/CS scaffolds and *A. wilhelmsii*-loaded scaffolds at the different incubation times

incubation, albeit with no statistical difference compared to the bare scaffold. The earlier degradation in the case of the loaded scaffolds (10 wt%) was observed to be 52.7% and 92% after 12 hr and 48 hr, respectively. At the same time, the rate of degradation was further accelerated for the loaded scaffolds containing 15 wt% extract and reached the peaks of 62.4% and 98%, which was insignificant compared to the 10 wt% extract-loaded scaffolds. Although the scaffolds covering the high content of the loaded extract (10 and 15 wt% extract) exhibited a higher degradation rate, possibly thanks to dropped polymer chain entanglements and enriched diffusion rate, all scaffolds were just about completely degraded after 72 hr in the controlled manner. Furthermore, this would be owing to more density of chemical binding between crosslinker and amine groups of CS and leads to gentler depolymerization [53].

Viability evaluations of cutaneous fibroblasts

The viability of HDF cells directly exposed to the scaffolds was determined at 24, 48, and 72 hr incubation, as shown in Fig. 7. First and foremost, the bare and loaded scaffolds not only had no cytotoxic effect but could also enhance cell viability and proliferation. Cells grown on the bare PVA/CS scaffold revealed a slightly increased viability (≥ 10%) compared to the control group after the three-time points. At 24 hr incubation, the cell viability was augmented to about 114% for 10 and 15 wt% extract-loaded scaffolds, more

than the control group. The results on the 48 hr incubation indicated the increasing growth of the cells so that the scaffold containing 5 wt% extract led to 110% viability, and even more cell growth (> 120%) appeared by the 10 wt% and 15 wt% extract-loaded scaffolds. Besides, no statistical difference was observed between the two scaffolds of 10% and 15 wt% extract, while a significant difference was for 5 wt% extract-loaded scaffold and particularly with the bare scaffold and control group. Likewise, at 72 hr incubation, cell proliferation reached 130% and 132% for 10% and 15wt% extract-loaded scaffolds, respectively. Therefore, *A. wilhelmsii*-loaded scaffolds with the concentrations of 10 wt% and 15 wt% exhibited excellent cell compatibility and enhanced the proliferation of dermal fibroblasts, which play a significant role in wound healing process. No significant variance was perceived in the cell-spreading zone among different incubation times based on the live/dead staining results. This outcome could be ascribed to the presence of growth-stimulating bioactive compounds in the extract [25, 54, 55].

In-vitro wound healing capability

The scratch assay was conducted to monitor the influence of the scaffolds on promoting the migration of HDF cells involved in wound healing. As exhibited in Fig. 8a, after 24 hr, 41% of the scratched area was filled with the cells and reached 65.8% after 48 hr so that a distinct
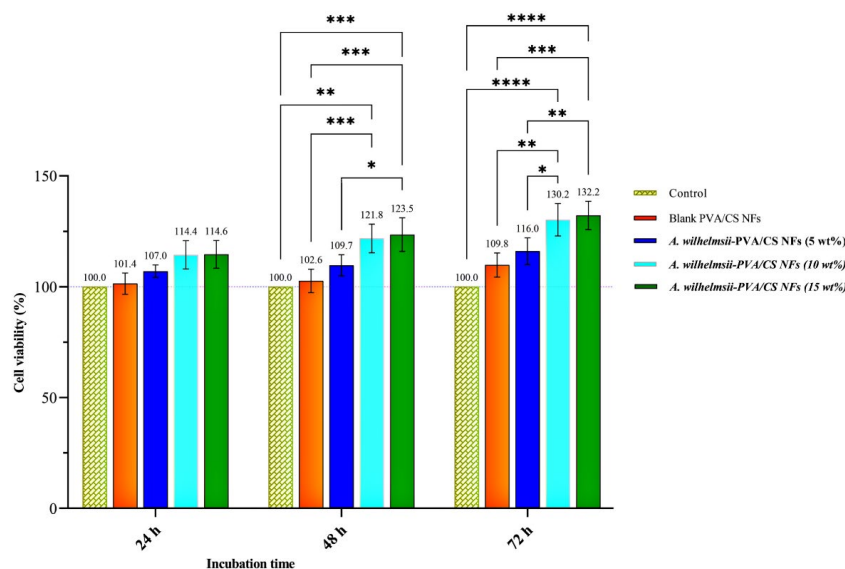
Fig. 7. Cell viability and proliferation of HDF cells on the prepared scaffolds at the different incubation times (*, **, ***, and **** indicate P<0.05, P<0.01, P<0.001, and P<0.0001, respectively)
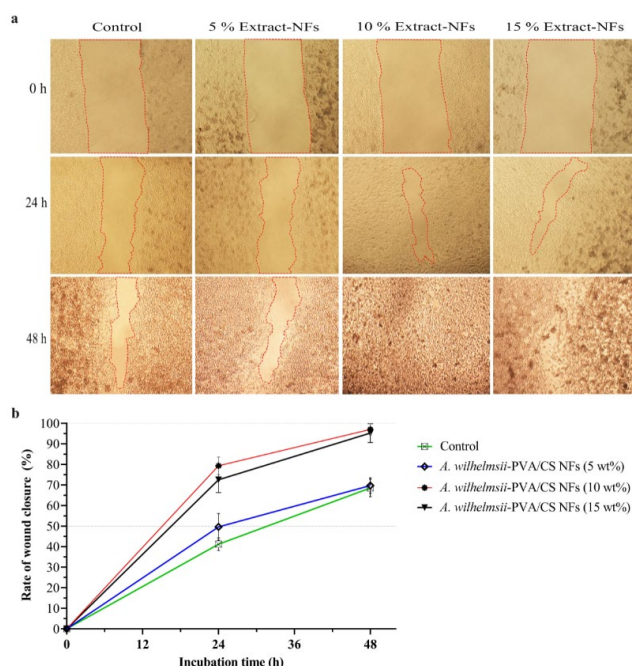
Fig. 8. a) Migration into a scratch area of dermal fibroblasts in the presence of nanofibrous scaffolds containing 5-15 wt% *A. wilhelmsii* extract relative to control group (without scaffold) over a 48 hr period (The resulting cell fronts are plotted in red); b) Quantitative wound closure relative to incubation time

zone remained free of the cell. The micrographs demonstrate that the scaffolds containing 5 wt% *A. wilhelmsii* extract stimulated cell migration and filled nearly 50% and 68% of the cell-free zone at 24 hr and 48 hr incubation, respectively, which was not significantly higher than those in the control (Fig. 8b). Particularly, the scaffold containing 10 wt% extract induced remarkable cell migration, resulting in 79% wound closure at 24 hr and the scratching gap was closed entirely after 48 hr. Likewise, 15 wt% extract-loaded scaffolds led to 72.5% after 24 hr and reached close to complete closure (95%) after 48 hr. The highest percentage of wound closure was observed in 10 wt% extract-loaded scaffolds, however, there was a significant difference with the control and 5 wt% extract-loaded scaffolds, as well as was no significant difference with 15 wt% extract-loaded scaffolds (Fig. 8b).

HDF migration is a crucial aspect of the healing of skin wounds and the formation of new tissue [56]. Thus, *A. wilhelmsii* contained the critical components that were liberated sustainably from the scaffolds capable of inducing cells to migrate in the wound area [57, 58]. The proposed scaffolds, specifically those containing 10 wt% *A. wilhelmsii* extract, could potentially lessen the inflammatory phase, enhance the proliferation phase, and promote the migration process.

CONCLUSION

The nanofibrous scaffolds composed of PVA/CS containing various contents of *A. wilhelmsii* extract were established for improving wound healing promotion. The electrospun-loaded scaffolds pointed out a nano-scale organized fibrous architecture with uniform morphology. Also, the relevant characterizations endorsed appropriate loading of *A. wilhelmsii* extract into the scaffold along with high porosity, water absorption, hydrophilicity, and mechanical strength. Besides, the controlled degradation over several days and the remarkable free-radical scavenging efficacy of scaffolds were verified. The viability studies affirmed the cytocompatibility and capacity to stimulate the proliferation of dermal fibroblasts. Also, the wound healing capability was specified with a significant accelerating fibroblast migration and comprehensive closure of scratched areas. As a result, this study offers the potential use of *A. wilhelmsii* extract-loaded PVA/CS NFs as a multifunctional scaffold for effectual wound healing applications.

ACKNOWLEDGMENTS

CONFLICTS OF INTEREST

The authors declare that they have no competing interests.

REFERENCES

1. Tottoli EM, Dorati R, Genta I, Chiesa E, Pisani S, Conti B. Skin wound healing process and new emerging technologies for skin wound care and regeneration. Pharmaceutics. 2020;12(8):735.
2. Gilaberte Y, Prieto-Torres L, Pastushenko I, Juarranz Á. Anatomy and Function of the Skin. In: Nanoscience in Dermatology. 2016:1-14. Academic Press.
3. Low ZWK, Li Z, Owh C, Chee PL, Ye E, Dan K, et al. Recent innovations in artificial skin. Biomater Sci. 2020;8(3):776–797.
4. Sorg H, Tilkorn DJ, Hager S, Hauser J, Mirastschijski U. Skin Wound Healing: An Update on the Current Knowledge and Concepts. Eur Surg Res. 2017;58(1–2):81–94.
5. Wilkinson HN, Hardman MJ. Wound healing: Cellular mechanisms and pathological outcomes. Open Biol. 2020;10(9):200223.
6. Singh S, Young A, McNaught CE. The physiology of wound healing. Surg. 2017;35(9):473–477.
7. Dreifke MB, Jayasuriya AA, Jayasuriya AC. Current wound healing procedures and potential care. Mater Sci Eng C. 2015;48:651–662.
8. Ovington LG. Advances in wound dressings. Clin Dermatol. 2007;25(1):33–38.
9. Dhivya S, Padma VV, Santhini E. Wound dressings - A review. Biomed. 2015;5(4):24–28.
10. Laurano R, Boffito M, Ciardelli G, Chiono V. Wound dressing products: A translational investigation from the bench to the market. In: Engineered Regeneration. 2022;3(2):182–200.
11. Kalva SN, Augustine R, Al Mamun A, Dalvi YB, Vijay N, Hasan A. Active agents loaded extracellular matrix mimetic electrospun membranes for wound healing applications. J Drug Deliv Sci Technol. 2021;63:102500.
12. Maleki H, Khoshnevisan K, Sajjadi-Jazi SM, Baharifar H, Doostan M, Khoshnevisan N, et al. Nanofiber-based systems intended for diabetes. J Nanobiotechnology. 2021;19:1-34.
13. Thenmozhi S, Dharmaraj N, Kadirvelu K, Kim HY. Electrospun nanofibers: New generation materials for advanced applications. Mater Sci Eng B Solid-State Mater Adv Technol. 2017;217:36–48.
14. Xue J, Wu T, Dai Y, Xia Y. Electrospinning and electrospun nanofibers: Methods, materials, and applications. Chem Rev. 2019;119: 5298–5415.
15. Liu Y, Zhou S, Gao Y, Zhai Y. Electrospun nanofibers as a wound dressing for treating diabetic foot ulcer. Asian J Pharm Sci. 2019;14(2):130–143.
16. Gonçalves MM, Lobsinger KL, Carneiro J, Picheth GF, Pires C, Saul CK, et al. Morphological study of electrospun chitosan/poly(vinyl alcohol)/glycerol nanofibres for skin care applications. Int J Biol Macromol. 2022;194:172–178.
17. Yang D, Li Y, Nie J. Preparation of gelatin/PVA nanofibers and their potential application in controlled release of drugs. Carbohydr Polym. 2007;69(3):538–543.
18. Sa'adon S, Abd Razak SI, Ismail AE, Fakhruddin K. Drug-Loaded Poly-Vinyl Alcohol Electrospun Nanofibers for Transdermal Drug Delivery: Review on Factors Affecting the Drug Release. Procedia Comput Sci. 2019;158:436–442.
19. Jin SG. Production and Application of Biomaterials Based on Polyvinyl alcohol (PVA) as Wound Dressing. Chem - An Asian J. 2022;17(21).
20. Wang W, Xue C, Mao X. Chitosan: Structural modification, biological activity and application. Int J Biol Macromol. 2020; 164:4532–4546.
21. Choi C, Nam JP, Nah JW. Application of chitosan and chitosan derivatives as biomaterials. J Ind Eng Chem. 2016;33: 1–10.
22. Abraham A, Soloman PA, Rejini VO. Preparation of chitosan-polyvinyl alcohol blends and studies on thermal and mechanical properties. Procedia Technol. 2016;24:741–748.
23. Saeidi K, Moosavi M, Lorigooini Z, et al. Chemical characterization of the essential oil compositions and antioxidant activity from Iranian populations of Achillea wilhelmsii K.Koch. Ind Crops Prod. 2018;112:274–280.
24. Kazemi M, Rostami H. Chemical composition and biological activities of Iranian Achillea wilhelmsii L. essential oil: A high effectiveness against Candida spp. and Escherichia strains. Nat Prod Res. 2015;29:286–288.
25. Afsharypuor S, Asgary S, Lockwood GB. Constituents of the essential oil of Achillea wilhelmsii from Iran. Planta Med. 1996;62:77–78.
26. Maleki H, Doostan M, Farzaei MH, et al. Achillea wilhelmsii–Incorporated Chitosan@Eudragit Nanoparticles Intended for Enhanced Ulcerative Colitis Treatment. AAPS PharmSciTech. 2023;24(5):112.
27. Chehrehgosha M, Khoshnevisan K, Maleki H, et al. A systematic study of nano-based fibrous systems: Diagnostic and therapeutic approaches for dementia control. Ageing Res Rev. 2023;85:101853.
28. Marjani ME, HMTShirazi R, Mohammadi T. CDI crosslinked chitosan/poly (vinyl alcohol) electrospun nanofibers loaded with Achillea millefolium and Viola extract: A promising wound dressing. Carbohydr Polym. 2024;336:122117.
29. Momtaz S, Azimian MA, Gharazi P, et al. The Hydro-alcoholic Extract of Achillea wilhelmsii C. Koch Ameliorates Acetic Acid-induced Ulcerative Colitis through TLR-4. Proc Natl Acad Sci India Sect B - Biol Sci. 2023;93:127–135.
30. Doostan M, Maleki H, Khoshnevisan K, Baharifar H, Doostan M, Bahrami S. Accelerating healing of infected wounds with G. glabra extract and curcumin Co-loaded electrospun nanofibrous dressing. J Biomater Appl. 2024; 08853282241252729.
31. Doostan M, Doostan M, Maleki H, Faridi Majidi R, Bagheri F, Ghanbari H. Co-electrospun poly(vinyl alcohol)/poly(ε-caprolactone) nanofiber scaffolds containing coffee and Calendula officinalis extracts for wound healing applications. J Bioact Compat Polym. 2022;37(6):437–52.
32. Doostan M, Doostan M, Mohammadi P, Khoshnevisan K, Maleki H. Wound healing promotion by flaxseed extract-loaded polyvinyl alcohol/chitosan nanofibrous scaffolds. Int J Biol Macromol. 2023;228:506–516.
33. Grada A, Otero-Vinas M, Prieto-Castrillo F, Obagi Z, Falanga V. Research Techniques Made Simple: Analysis of Collective Cell Migration Using the Wound Healing Assay. J Invest Dermatol. 2017;137(2):e11–16.
34. Unalan I, Endlein SJ, Slavik B, Buettner A, Goldmann WH, Detsch R, et al. Evaluation of electrospun poly(ε-caprolactone)/gelatin nanofiber mats containing clove essential oil for antibacterial wound dressing. Pharmaceutics. 2019;11(11):570.
35. Shenoy SL, Bates WD, Frisch HL, Wnek GE. Role of chain entanglements on fiber formation during electrospinning of polymer solutions: Good solvent, non-specific polymer-polymer interaction limit. Polymer (Guildf).

2005;46(10):3372–3384.

36. Majumder S, Matin MA, Sharif A, Arafat MT. Understanding solubility, spinnability and electrospinning behaviour of cellulose acetate using different solvent systems. Bull Mater Sci. 2019;42(4):171.

37. Maleki H, Doostan M, Khoshnevisan K, Baharifar H, Maleki SA, Fatahi MA. Zingiber officinale and thymus vulgaris extracts co-loaded polyvinyl alcohol and chitosan electrospun nanofibers for tackling infection and wound healing promotion. Heliyon. 2024;10(1).

38. Asariha M, Chahardoli A, Karimi N, Gholamhosseinpour M, Khoshroo A, Nemati H, et al. Green synthesis and structural characterization of gold nanoparticles from Achillea wilhelmsii leaf infusion and in vitro evaluation. Bull Mater Sci. 2020;43:1-10.

39. Soneja A, Drews M, Malinski T. Role of nitric oxide, nitroxidative and oxidative stress in wound healing. Pharmacol Reports. Pharmacol Reports. 2005;57:108.

40. Schäfer M, Werner S. Oxidative stress in normal and impaired wound repair. Pharmacol Res. 2008;58:165–171.

41. Alfatemi SMH, Sharifi-Rad JS, Rad MS, Mohsenzadeh S, da Silva JAT. Chemical composition, antioxidant activity and in vitro antibacterial activity of Achillea wilhelmsii C. Koch essential oil on methicillin-susceptible and methicillin-resistant Staphylococcus aureus spp. 3 Biotech. 2015;5(1):39–44.

42. Comino-Sanz IM, López-Franco MD, Castro B, Pancorbo-Hidalgo PL. The role of antioxidants on wound healing: A review of the current evidence. J Clin Med. 2021;10(16):3558.

43. Do Nascimento LD, de Moraes AAB, da Costa KS, Galúcio JMP, Taube PS, Costa CML, et al. Bioactive natural compounds and antioxidant activity of essential oils from spice plants: New findings and potential applications. Biomolecules. 2020;10(7):1–37.

44. Süntar I., Akkol E. K., Nahar L., Sarker S. D. Wound healing and antioxidant properties: do they coexist in plants? Free Radicals Antioxidants. 2012;2(2):1-7.

45. Udenni Gunathilake TMS, Ching YC, Ching KY, Chuah CH, Abdullah LC. Biomedical and microbiological applications of bio-based porous materials: A review. Polymers (Basel). 2017;9(5):160.

46. Sheik S, Sheik S, Nairy R, Nagaraja GK, Prabhu A, Rekha PD, et al. Study on the morphological and biocompatible properties of chitosan grafted silk fibre reinforced PVA films for tissue engineering applications. Int J Biol Macromol. 2018;116:45–53.

47. Negut I, Dorcioman G, Grumezescu V. Scaffolds for wound healing applications. Polymers (Basel). 2020;12(9):1–19.

48. Liu X, Xu H, Zhang M, Yu DG. Electrospun medicated nanofibers for wound healing: Review. Membranes (Basel). 2021;11(10):770.

49. Nemati S, Kim S jeong, Shin YM, Shin H. Current progress in application of polymeric nanofibers to tissue engineering. Nano Converg. 2019;6(1):36.

50. Fathi A, Khanmohammadi M, Goodarzi A, Foroutani L, Mobarakeh ZT, Saremi J, et al. Fabrication of chitosan-polyvinyl alcohol and silk electrospun fiber seeded with differentiated keratinocyte for skin tissue regeneration in animal wound model. J Biol Eng. 2020;14(1):27.

51. Sharma S, Gupta A, Rath G, Goyal A, Mathur RB, Dhakate SR. Electrospun composite nanofiber-based transmucosal patch for anti-diabetic drug delivery. J Mater Chem B. 2013;1(27):3410–3418.

52. Kajdič S, Planinšek O, Gašperlin M, Kocbek P. Electrospun nanofibers for customized drug-delivery systems. J Drug Deliv Sci Technol. 2019;51:672–681.

53. Berger J, Reist M, Mayer JM, Felt O, Peppas NA, Gurny R. Structure and interactions in covalently and ionically crosslinked chitosan hydrogels for biomedical applications. Eur J Pharm Biopharm. 2004;57(1):19–34.

54. Saeidnia S, Gohari AR, Mokhber-Dezfuli N, Kiuchi F. A review on phytochemistry and medicinal properties of the genus Achillea. DARU, J Pharm Sci. 2011;19(3):173–186.

55. Mohammadhosseini M, Sarker SD, Akbarzadeh A. Chemical composition of the essential oils and extracts of Achillea species and their biological activities: A review. J Ethnopharmacol. 2017;199:257–315.

56. Sukum P, Punyodom W, Dangtip S, Poramapijitwat P, Daranarong D, Jenvoraphot T, et al. Argon Plasma Jet-Treated Poly (Vinyl Alcohol)/Chitosan and PEG 400 Plus Mangifera indica Leaf Extract for Electrospun Nanofiber Membranes: In Vitro Study. Polymers (Basel). 2023;15(11):2559.

57. Akbari B, Baghaei-Yazdi N, Bahmaie M, Mahdavi Abhari F. The role of plant-derived natural antioxidants in reduction of oxidative stress. BioFactors. 2022;48(3):611–633

58. Koushki M, Farrokhi Yekta R, Amiri-Dashatan N, Dadpay M, Goshadrou F. Therapeutic effects of hydro-alcoholic extract of Achillea wilhelmsii C. Koch on indomethacin-induced gastric ulcer in rats: A proteomic and metabolomic approach. BMC Complement Altern Med. 2019;19:1-16.